ELSEVIER

Journal of Non-Crystalline Solids 202 (1996) 201–202

Upconversion fluorescence and low temperature fluorescence properties in Nd^{3+}-doped $ZnCl_2$-based glass

Takashi Tsuneoka, Kazuo Kojima *, Sreedhar Bojja

Department of Chemistry, Ritsumeikan University, 1916 Nojihi-cho, Kusatsu, Shiga 525, Japan

Received 14 June 1995; revised 23 January 1996

Abstract

A Nd^{3+}-doped $ZnCl_2$-based glass sample was prepared by quenching its liquid in a glass tube. Upconversion fluorescence due to Nd^{3+} ion observed in the UV to visible region (360, 385, 415, 433, 480, 520, 532, 575, 592, 650, 695 and 805 nm) by laser diode excitation. Some of the emission were assigned by measuring normal fluorescence and excitation spectra at room temperature. Moreover, upconversion and normal fluorescence of this glass were also measured at liquid nitrogen temperature. The evolution behaviour in this glass was discussed by comparing spectra measured at room and low temperatures.

1. Introduction

Recently, many studies have been done on upconversion fluorescence in various glasses doped with rare earth ions such as Er^{3+} [1,2]. The upconversion fluorescence phenomenon, i.e., conversion of excitation light to shorter wavelength light, has been essential for applications in infrared-pumped short-wavelength solid state lasers. Among several glasses, fluoride glasses have attracted considerable attention because of their high upconversion efficiencies. This higher efficiency is because the phonon energies in fluoride glasses are less than in oxide glasses and reduce nonradiative losses due to multiphonon relaxation. In chloride glasses such as $ZnCl_2$-based systems, transmission of light in the far-IR region is superior to that of fluoride glasses because of low vibrational frequencies between glass-forming cation such as Zn^{2+} and chloride ion, Cl^- [3,4]. $ZnCl_2$ is the best glass former among chlorides and its structure is well investigated [4–6]. From Raman spectroscopy [3,7], chloride glasses were found to have lower vibrational frequencies than fluoride glasses, the frequency of the Zn–Cl symmetric stretching mode being only 230–280 cm^{-1}. Therefore, excellent emission efficiencies are expected for chloride glasses due to their lower phonon energies, in spite of the difficulty in glass properties arising from strong hygroscopicity of chlorides. In fact, Ghanavi and McPherson [8] reported the visible to UV upconversion in Er^{3+}-doped $ZnCl_2$- and $CdCl_2$-based glasses for the first time. Quite recently, the near-IR to visible upconversion was first observed in similar systems by Shojiya et al. [9].

In Nd^{3+}-doped crystalline and glassy materials, many fundamental and applied studies concerning

* Corresponding author. Tel.: +81-775 61 2111; fax: +81-775 61 2599; e-mail: kojima@ritsumei.ac.jp.

PII 0022-3093(96)00196-4

1064 nm laser emission due to the $^4F_{3/2} \rightarrow {}^4I_{11/2}$ transition have been carried out in order to search for laser materials having better optical properties. Especially, in various glassy hosts, systematic studies of this emission have been mainly done because glassy hosts have the possibility of high-power laser oscillation and because their preparation and variation in composition are relatively easy compared with crystalline hosts [10–12]. As for upconversion of Nd^{3+} ion, upconversion fluorescence and upconversion laser emission have been reported in oxide and fluoride single crystals such as $Y_3Al_5O_{12}$(YAG), LaF_3 and $YLiF_4$ under high-power laser excitations of various wavelengths [13–18]. Upconversion fluorescence in Nd^{3+}-doped glasses had not been detected until quite recently; Stanley et al. [19] first observed UV and visible upconversion fluorescence in Nd^{3+}-doped fluoride glasses under near-IR laser diode excitation. They assigned the complicated visible emission bands and suggested possible mechanisms for two- and three-photon excitation processes. To our knowledge, there has been no report on upconversion fluorescence in Nd^{3+}-doped chloride glasses.

In the present work, we prepared a Nd^{3+}-doped $ZnCl_2$-based glass and observed its UV and visible upconversion fluorescence for the first time under near-IR excitation. This paper also discusses the emission behaviour in this glass by comparing the spectra examined at room and liquid nitrogen temperatures.

2. Experimental

High-purity chlorides were used as starting materials after being dried under vacuum because of their strong hygroscopicity. After weighing and mixing in a glove box purged with N_2 gas, the powdered mixture was dehydrated again under vacuum. The composition of the batch mixture was $79.5ZnCl_2$–$10KCl$–$10BaCl_2$–$0.5NdCl_3$ in molar ratio. A small amount of NH_4Cl was added to the mixture to remove residual water. The dried mixture was quickly put into a glass tube of 5 mm inside diameter in the glove box and then melted at about 450°C for approximately 30 min under N_2 or Ar atmosphere. Residual impurities in the liquid, such as water and NH_4Cl, were removed by evacuation. A glass sample was obtained by quenching the glass tube containing the liquid below 0°C. Then, liquid paraffin was poured into the glass tube to prevent exposing the glass sample to air. All optical measurements were carried out with the samples being kept in the glass tubes. The upconversion fluorescence spectrum was examined using an optical system consisting mainly of a monochromator (Nikon G-250) [0.1 nm resolution] equipped with a R-376 photomultiplier (Hamamatsu Photonics) and an AlGaAs laser diode (Sony SLD-302V-24, 805 nm, 72 mW) as an excitation source (Fig. 1). The fluorescence and excitation spectra were examined with a fluorescence spectrophotometer (Hitachi F-4500) (1 nm resolution) at room temperature. In order to take the upconversion fluorescence at 77 K, an intermediate Dewar flask was used. The normal fluorescence spectrum at 77 K was recorded on the optical system shown in Fig. 1 by exciting the sample with monochromatic light from a 800 W Xe-lamp instead of the laser diode.

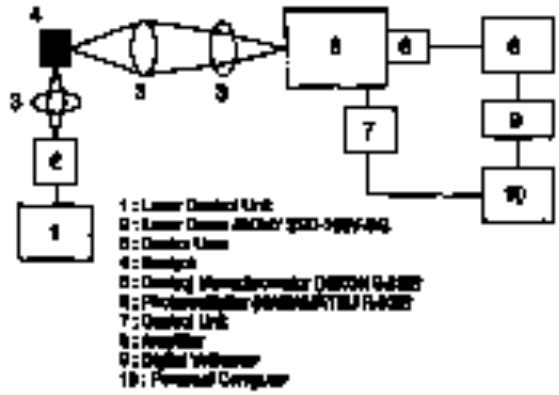

Fig. 1. Schematic diagram of an optical system for the upconversion fluorescence measurement.

3. Results

3.1. Upconversion fluorescence properties at room temperature

Fig. 2(a) and (c) show upconversion fluorescence spectra of a Nd^{3+}-doped $ZnCl_2$-based glass at room temperature. As can be seen, upconverted emission bands were first observed for chloride glasses in the UV to visible region (340, 365, 415, 453, 480, 520, 532, 575, 595, 650, 661 nm) under 805 nm laser diode

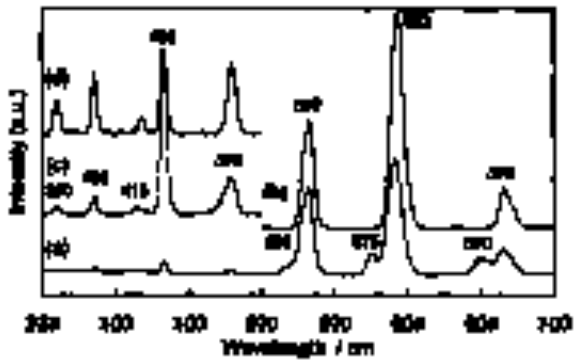

Fig. 2. Upconversion fluorescence spectra of a Nd^{3+}-doped $ZnCl_2$-based glass sheet: 800 nm excitation at room (a, c) and liquid nitrogen (b, d) temperatures.

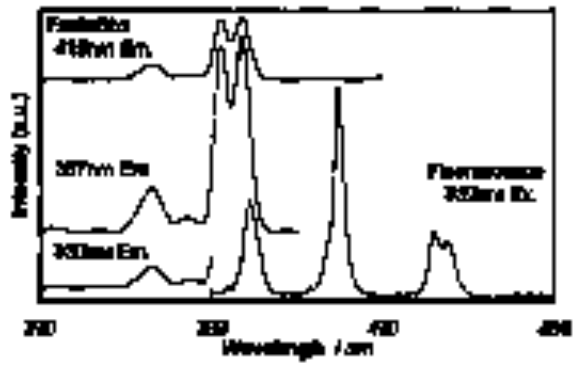

Fig. 4. Normal fluorescence and excitation spectra in the short-wavelength range.

excitation, being similar to those of fluoride glasses [19]. Yellow emission at 582 nm was strong enough to be clearly seen by the naked eye.

The dependence of these fluorescence intensities on the 800 nm excitation power is shown in Fig. 3. The intensities of the emissions with wavelengths longer than 433 nm increase almost in proportion to the square of the excitation power. On the other hand, the intensities of the 360, 385, and 415 nm peaks have the dependence with an exponent 2.3–2.5, being greater than 2. As mentioned by Stanley et al. [19], these three emissions are assumed to result from a three-photon excitation process. They are also detected in the normal fluorescence under 330 nm excitation, as shown in Fig. 4. Though the emissions originating from the $^2P_{3/2}$ state, the $^2P_{3/2} \rightarrow {}^4I_{9/2}$ (383 nm) and $^2P_{3/2} \rightarrow {}^4I_{11/2}$ (413 or 414 nm) transitions have been observed in crystalline hosts such as YLiF$_4$ [17,18], it is concluded from excitation spectra for each emission (see Fig. 4) that the emissions in the present chloride glass arise from the common state ($^4D_{3/2}$) and assigned as follows: 360 nm, $^4D_{3/2} \rightarrow {}^4I_{9/2}$ (ground state); 385 nm, $^4D_{3/2} \rightarrow {}^4I_{11/2}$ (first excited state); and 415 nm, $^4D_{3/2} \rightarrow {}^4I_{13/2}$ (second excited state). These components are shown in Fig. 5.

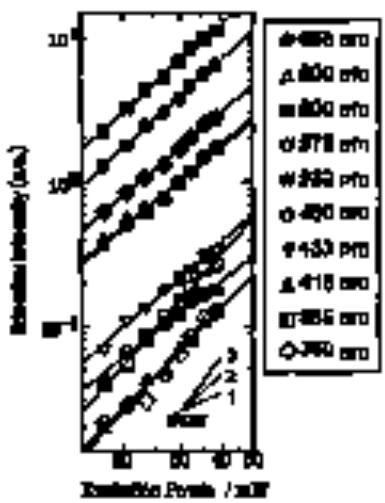

Fig. 3. Excitation power dependences of various upconversion fluorescence intensities.

3.2. Low temperature fluorescence properties

Upconversion fluorescence spectra at 77 K are shown in Fig. 2(b) and (d). The 520 nm shoulder and the two emissions at 575 and 680 nm are found to be quenched. Each of the quenched (650 nm) and non-quenched (685 nm) emissions is assigned to be due to the transition between two excited states because there are no energy levels of Nd^{3+} ion corresponding to these energies from the ground state. In order to clarify the mechanism of these emissions, normal fluorescence and excitation spectra were examined. First, normal fluorescence was measured at room temperature under excitation in the region of 510–535 nm ($^2G_{9/2}$, $^4G_{7/2}$ levels) and 575–590 nm ($^4G_{5/2} + {}^2G_{7/2}$ levels), as shown in Fig. 6. As can be seen from the spectra at room temperature, the former type of excitation gives both of the 650 and 685 nm bands that have the same spectral profiles as

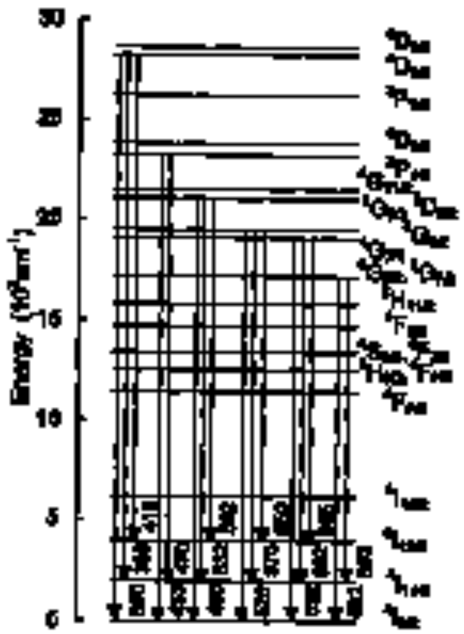

Fig. 6. Energy level diagram of Nd^{3+} with the assignments of upconversion emission bands.

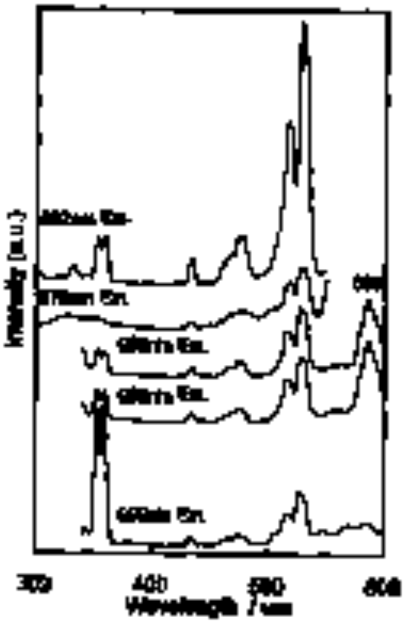

Fig. 7. Excitation spectra of the 377, 592, 650, 663 and 665 nm emissions.

upconversion fluorescence at room temperature, while the latter type of excitation gives only the broad 653 nm band slightly shifted to shorter wave-

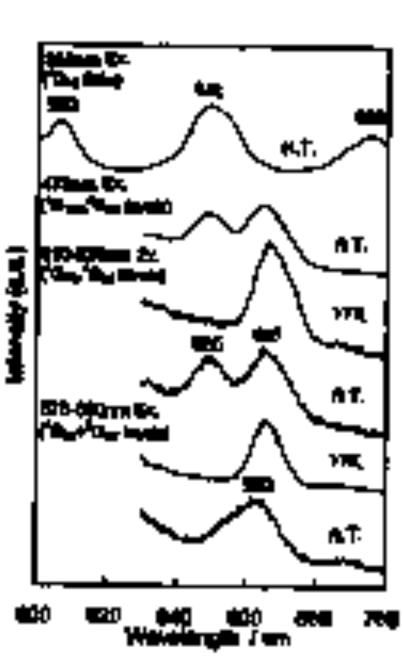

Fig. 8. Partial fluorescence spectra in the range of 600–700 nm under excitation of various wavelengths.

length side. In the excitation spectra for these emissions (see Fig. 7), each of the 663 and 665 nm emissions exhibits the peak corresponding to the $^4I_{9/2} \rightarrow {}^4G_{5/2} + {}^2G_{7/2}$ transition at about 588 nm, whereas the 650 nm emission does not show it.

4. Discussion

4.1. Assignments of some upconverted emission bands

In contrast with the fact that the assignments of emission bands in the short-wavelength range are relatively simple, the visible emissions in the longer-wavelength region are too complicated to be interpreted because there are many energy levels of Nd^{3+} ion and many possible transitions from one excited state to other lower excited states. In this work, we attempt to assign some of the visible emissions by measuring low temperature fluorescence spectra.

First the mechanisms of the 650, 653 and 665 nm emissions in Fig. 6 are discussed. From excitation

spectra in Fig. 7, it is considered that the 650 nm emission is originating from the higher energy levels than the $^4G_{5/2}+{}^2G_{7/2}$ levels. The 600 and 695 nm emissions are too broad to distinguish their transitions clearly from excitation spectra. However, the 600 nm band can be attributed to the $^4G_{5/2}+{}^2G_{7/2} \rightarrow {}^4I_{13/2}$ transition from the fluorescence spectra under 575–590 nm excitation ($^4G_{5/2}+{}^2G_{7/2}$ levels) in Fig. 6 and its assignment is different from that of the 600 nm emission band. Therefore, this 695 nm band is also assigned to originate from energy levels higher than the $^4G_{5/2}+{}^2G_{7/2}$ levels. By considering a combination of the energy gap of 350 cm^{-1} between the 650 and 695 nm emissions and the energy level diagram of Nd^{3+} ion, the quenched (650 nm) and unquenched (695 nm) emissions are probably assigned to the $^4G_{9/2} \rightarrow {}^4I_{13/2}$ and $^4G_{7/2} \rightarrow {}^4I_{13/2}$ transitions, respectively. That is to say, it is likely that at room temperature the $^4G_{9/2}$ level can be thermally populated from the underlying low-energy emissible level $^4G_{7/2}$, whereas this is not likely at 77 K. As shown in Fig. 6, the 650 nm emission is also quenched at 77 K under 510–533 nm excitation in normal fluorescence as well as in upconversion fluorescence. This fact supports the result that the $^4G_{9/2}$ level has less population at 77 K.

Second, the quenched 520 and 575 nm emissions in Fig. 2 will be discussed from the viewpoint of energy level gap of Nd^{3+} ion. When both the 520 and 650 nm emission bands originate from the $^4G_{9/2}$ level, they give an energy gap value of 3850 cm^{-1} between the $^4I_{13/2}$ and $^4I_{9/2}$ levels, being comparable with that of 3680 cm^{-1} calculated from the obvious 360 and 415 nm bands originating from the $^4D_{3/2}$ level. Similarly, as a gap between the $^4I_{11/2}$ and $^4I_{9/2}$ levels, the 520 and 575 nm emission bands give 1845 cm^{-1}, being in agreement with 1800 cm^{-1} derived from the 360 and 385 nm bands. Consequently, the quenched 520 and 575 nm emissions are considered to be originating from the $^4G_{9/2}$ level that is the same initial level as the quenched 650 nm emission and assigned to the $^4G_{9/2} \rightarrow {}^4I_{9/2}$ and $^4G_{9/2} \rightarrow {}^4I_{11/2}$ transitions, respectively.

4.1. Other possible assignments of emission bands

The foregoing discussion from the viewpoint of energy level gap of Nd^{3+} ion is also applicable to other emissible levels. Considering the emissions from the $^4G_{7/2}$ level, the transitions to the $^4I_{9/2}$ and $^4I_{11/2}$ levels correspond to the 532 and 592 nm emissions, respectively. Actually, these two emissions are strongly detectable in upconversion fluorescence as shown in Fig. 2(a). The 592 nm emission is also expected for the $^4G_{5/2}+{}^2G_{7/2} \rightarrow {}^4I_{9/2}$ and $^4G_{9/2} \rightarrow {}^4I_{11/2}$ transitions in the same way. These possible assignments of observed emission bands are summarized in Fig. 5.

Then, possible transitions from the energy levels higher than the $^4G_{9/2}$ and $^4G_{7/2}$ levels will be discussed. In the excitation spectra for the 650 nm emission, the peaks corresponding to the $^4D_{9/2} \rightarrow {}^4I_{9/2,11/2}$ transitions around 355 nm are observed in comparison with those for the 695 and 695 nm emissions (see Fig. 7). In fact, normal fluorescence spectrum under the 358 nm ($^4D_{3/2}$ level) excitation at room temperature gives the 649 nm and weak band in addition to the 600 and 695 nm emission bands. These emissions are attributed to the transitions originating from the common state $^4D_{9/2}$ and assigned as $^4D_{3/2} \rightarrow {}^4F_{3/2}$ (696 nm), $^4D_{3/2} \rightarrow {}^2H_{9/2}+{}^4F_{5/2}$ (649 nm) and $^4D_{9/2} \rightarrow {}^4S_{3/2}+{}^4F_{9/2}$ (600 nm), because they are not observed under the excitation at the energy levels less than the $^4D_{9/2}$ level. This 649 nm emission band is assumed to differ from the quenched emission (650 nm), the reasons of which are as follows. Provided the quenched emission (650 nm) in upconversion fluorescence is due to the transition from the $^4D_{3/2}$ level, the emission should result from a three-photon excitation process and therefore the slope in Fig. 3 should be greater than 2. Moreover, the 600 and 695 nm emissions shown in Fig. 6 should also be observed in upconversion fluorescence at room temperature. The quenched emission (650 nm), however, is obviously resulting from a two-photon excitation process and the 600 and 695 nm emissions are not observed as shown in Fig. 2(a). Consequently, it is easily understandable that the 649 nm emission from the $^4D_{3/2}$ level is different from the quenched emission (650 nm).

As a combination of the quenched (650 nm) and unquenched (695 nm) emissions, it may be presumed that the transitions from the $^4G_{11/2}$ and $^2G_{9/2}$ levels are possible. The energy gap between the $^4G_{11/2}$ and $^2G_{9/2}$ levels is 350 cm^{-1}, being comparable with that between the $^4G_{9/2}$ and $^4G_{7/2}$ levels. The $^4G_{11/2}$

and $^2G_{9/2}$ levels, moreover, are higher-lying levels by 2000 cm^{-1} than the $^4G_{9/2}$ and $^4G_{7/2}$ levels. This value corresponds to the energy gap between the neighbouring lower-lying levels (i.e., $^4I_{9/2}$–$^4I_{15/2}$) of Nd^{3+} ion. Therefore, it is possible that the 650 and 666 nm emissions are assigned to the $^4G_{11/2} \rightarrow ^4I_{15/2}$ and $^2G_{9/2} \rightarrow ^4I_{15/2}$ transitions, respectively. In the normal fluorescence spectrum under the 473 nm ($^4G_{11/2}$, $^2G_{9/2}$ levels) excitation at room temperature, the 650 and 666 nm emissions having the same spectral profiles as that under 510–535 nm ($^4G_{9/2}$, $^4G_{7/2}$ levels) at room temperature are observed as shown in Fig. 6. These emissions are considered to be resulting from nonradiative relaxation into the $^4G_{9/2}$ and $^4G_{7/2}$ levels from the $^4G_{11/2}$ and $^2G_{9/2}$ levels, although the transitions from the $^4G_{11/2}$ and $^2G_{9/2}$ levels cannot still be excluded. By considering that the 470 nm shoulder quenches in upconversion fluorescence at 77 K as shown in Fig. 2(d), it is understandable that no emissions from the $^4G_{11/2}$ level take place at 77 K, and that the foregoing transitions from the $^4G_{11/2}$ and $^2G_{9/2}$ levels are possible. The 470 nm emission shall also be observed due to the $^2P_{1/2} \rightarrow ^4I_{11/2}$ transition having the same initial level as the 433 nm emission level. The emissions from the $^2P_{1/2}$ level have been reported in fluoride glasses [10], being assigned as $^2P_{1/2} \rightarrow ^4I_{15/2}$ (313 nm) and $^2P_{1/2} \rightarrow ^4I_{11/2}$ (572 nm). In the present study, the intensities of the emissions from the $^2P_{1/2}$ level (433, 470 nm) are found to be decreased at 77 K as shown in Fig. 2; however, the reason is not clear at the present stage.

5. Conclusions

A Nd^{3+}-doped $ZnCl_2$-based glass was prepared by quenching its liquid in a glass tube. Upconversion fluorescence due to Nd^{3+} was first observed for chloride glasses in the UV to visible region under 800 nm laser diode excitation. Some of the complicated visible emissions were assigned by comparing normal and upconversion fluorescence spectra at room and liquid nitrogen temperatures. The quenched (650 nm) and unquenched (666 nm) emissions at liquid nitrogen temperature were assigned to the $^4G_{9/2} \rightarrow ^4I_{13/2}$ and $^4G_{7/2} \rightarrow ^4I_{11/2}$ transitions, respectively. We concluded that the $^4G_{9/2}$ level was thermally populated from the underlying $^4G_{7/2}$ level at room temperature.

Acknowledgements

Mr M. Yamazaki and Mr H. Yamada are gratefully acknowledged for setting up the optical system shown in Fig. 1.

References

[1] D.C. Yeh, W.A. Sibley, M. Suscavage and M.G. Drexhage, J. Appl. Phys. 62 (1987) 266.
[2] S. Tanabe, K. Hirao and N. Soga, J. Non-Cryst. Solids 122 (1990) 79.
[3] J. Lucas and J.-L. Adam, Glastech. Ber. 62 (1989) 422.
[4] R.M. Almeida and J.D. Mackenzie, J. Am. Ceram. Soc. 77 (1994) 2669.
[5] K. Kitagawa, K. Kadono and H. Tanaka, J. Non-Cryst. Solids 180 (1994) 285.
[6] K. Kadono, K. Kitagawa and H. Tanaka, Phys. Chem. Glasses 34 (1993) 59.
[7] K. Kadono, T. Shimomura and H. Tanaka, Phys. Chem. Glasses 32 (1991) 28.
[8] A. Ghiretti and D.L. McPherson, Appl. Phys. Lett. 61 (1992) 2635.
[9] M. Shojiya, M. Takahashi, R. Kanno, Y. Kawamoto and K. Kadono, Appl. Phys. Lett. 65 (1994) 1874.
[10] M.J. Weber, R.A. Saroyan and R.C. Ropp, J. Non-Cryst. Solids 44 (1981) 137.
[11] T. Kanazawa, H. Tomomi and H. Kawazoe, J. Non-Cryst. Solids 47 (1982) 87.
[12] M.J. Weber, D.C. Ziegler and C.A. Angell, J. Appl. Phys. 53 (1982) 4344.
[13] J. Alegre, B. Jacquier, C. Fabric and G. Boulon, Mater. Chem. Phys. 21 (1989) 217.
[14] B.R. Reddy and P. Venkateswarlu, J. Chem. Phys. 79 (1983) 5845.
[15] R.M. Macfarlane, F. Tong, A.J. Silversmith and W. Lenth, Appl. Phys. Lett. 52 (1988) 1300.
[16] T.Y. Fan and R.L. Byer, J. Opt. Soc. Am. B3 (1986) 1519.
[17] W. Lenth and R.M. Macfarlane, J. Lumin. 45 (1990) 346.
[18] M. Malinowski, B. Jacquier, M. Bouazaoui, M.F. Joubert and C. Linarès, Phys. Rev. B41 (1990) 31.
[19] A.T. Stanley, E.A. Harris, T.M. Searle and J.M. Parker, J. Non-Cryst. Solids 161 (1993) 235.